Astronomy & Astrophysics manuscript no. output
March 19, 2026

HOLISMOKES XIX: SN 2025wny at $z = 2$, the first strongly lensed superluminous supernova

Stefan Taubenberger[1,2], Ana Acebron[3,4], Raoul Cañameras[5], Ting-Wan Chen[6], Aymeric Galan[2,1], Claudio Grillo[7,4], Alejandra Melo[2,1], Stefan Schuldt[7,4], Allan G. Schweinfurth[1,2], Sherry H. Suyu[1,2], Greg Aldering[8], Amar Aryan[6], Yu-Hsing Lee[6], Elias Mamuzic[2,1], Martin Millon[9,10], Thomas M. Reynolds[11,12,17], Alexey V. Sergeyev[13,14], Ildar M. Asfandiyarov[15], Stéphane Basa[5], Stéphane Blondin[16,5], Otabek A. Burkhonov[15], Lise Christensen[17,12], Frederic Courbin[18,19,20], Shuhrat A. Ehgamberdiev[15,21], Tom L. Killestein[22], Seppo Mattila[11,23], Asadulla M. Shaymanov[15], Yiping Shu[24], Dong Xu[25], Sheng Yang[26], Daniel Gruen[27,28], Justin D. R. Pierel[29,30], Christopher J. Storfer[31], Kim-Vy Tran[32] Kenneth C. Wong[33], Rosa L. Becerra[34], Damien Dornic[35], Jean-Grégoire Ducoin[35], Noémie Globus[36], Claudia P. Gutiérrez[20,37], Ji-an Jiang[38,39], Hanindyo Kuncarayakti[11], Diego López-Cámara[40], Peter Lundqvist[41], Francesco Magnani[35], Enrique Moreno Méndez[42], Benjamin Schneider[5], Christian Vogl[2,1]

(Affiliations can be found after the references)

Received XX XX, 2025

ABSTRACT

We present imaging and spectroscopic observations of supernova SN 2025wny, associated with the lens candidate PS1 J0716+3821. Photometric monitoring from the Lulin and Maidanak observatories confirms multiple point-like images, consistent with SN 2025wny being strongly lensed by two foreground galaxies. Optical spectroscopy of the brightest image with the Nordic Optical Telescope and the University of Hawaii 88-inch Telescope allowed us to determine the redshift to be $z_{\rm SN} = 2.008 \pm 0.001$, based on narrow absorption lines originating in the interstellar medium of the supernova host galaxy. At this redshift, SN 2025wny shows a very high rest-frame UV flux and broad spectral features even weeks after the explosion, which is consistent with superluminous supernovae of Type I. We find a high ejecta temperature and depressed spectral lines compared to other similar objects. We also measured, for the first time, the redshift of the fainter of the two lens galaxies (the 'perturber') to be $z_{\rm p} = 0.375 \pm 0.001$, which is fully consistent with the DESI spectroscopic redshift of the main deflector at $z_{\rm d} = 0.3754$. Thus, SN 2025wny represents the first confirmed galaxy-scale strongly lensed supernova with time delays likely in the range of days to weeks, as judged from the image separations. This makes SN 2025wny suitable for cosmography, offering a promising new system for independent measurements of the Hubble constant. Following a tradition in the field of strongly lensed supernovae, we give SN 2025wny the nickname SN Winny.

Key words. Supernovae: general – Supernovae: individual: SN 2025wny – Cosmology: distance scale – Gravitational lensing: strong

1. Introduction

The persistent tension in measurements of the Hubble constant, H_0, most notably between the local distance ladder using Type Ia supernovae (SNe) from SH0ES (e.g. Riess et al. 2022) and early Universe inferences from Planck cosmic microwave background observations (Planck Collaboration et al. 2020), highlights both gaps in our understanding of cosmology and the need for independent probes (e.g. Moresco et al. 2022; Verde et al. 2024). Astrophysical transients, such as SNe, that are strongly lensed by foreground galaxies or galaxy clusters into multiple, time-delayed images offer a particularly powerful way to measure H_0 and other cosmological parameters (Refsdal 1964). The time delays between the multiple transient images together with a lens model of the total mass distribution, yield a direct measurement of the time-delay distance (Suyu et al. 2010) and hence H_0, which is independent of both the distance ladder and early Universe measurements (see recent reviews by e.g. Oguri 2019; Treu et al. 2022; Suyu et al. 2024)

Due to the rarity of strongly lensed SNe, the time-delay method has been demonstrated through lensed quasars instead, which are more abundant (e.g. Suyu et al. 2017; Wong et al. 2020; Birrer et al. 2020; Millon et al. 2020; Tdcosmo Collaboration et al. 2025). The past decade has seen rapid progress in the discovery of strongly lensed supernovae following the first detection of SN Refsdal (Kelly et al. 2015). Since then, the number of known systems has grown to nearly ten; most of these SNe are lensed by galaxy clusters (e.g. Rodney et al. 2021; Chen et al. 2022; Frye et al. 2023; Pierel et al. 2024), and only two systems are lensed by individual galaxies (Goobar et al. 2017, 2023). Three of the galaxy-cluster systems have yielded the first H_0 measurements from lensed SNe (Kelly et al. 2023; Grillo et al. 2024; Liu & Oguri 2025; Pascale et al. 2025; Pierel et al. 2025; Suyu et al. 2025; Agrawal et al. 2025). The two previously known galaxy-scale systems, iPTF16geu and SN Zwicky, had short time delays of $\lesssim 1$ day (Dhawan et al. 2020; Pierel et al. 2023), which were not suitable for precision cosmography.

With lensed SNe becoming an observational reality, we initiated the HOLISMOKES programme (Highly Optimised Lensing Investigations of Supernovae, Microlensing Objects, and Kinematics of Ellipticals and Spirals; Suyu et al. 2020). The goals of the programme are to (1) measure the Hubble constant through the lensing time delays of SNe and (2) constrain the properties

Article published by EDP Sciences, to be cited as https://doi.org/10.1051/0004-6361/202557847

of SN progenitors by using lensing time delays as a cosmic time machine, enabling early phase observations of trailing SN images soon after their explosion.

Not only are lensed SNe an excellent probe of cosmology and SN progenitors, but the lensing effect also provides an amplified SN flux and a magnified view of their host galaxies. In fact, lensing clusters and galaxies have been used as natural cosmic telescopes to study distant sources that would otherwise be too faint to be observed with existing facilities (e.g. Vanzella et al. 2017; Meštrić et al. 2023; Messa et al. 2025). As an example, Dhawan et al. (2024) showed that SN Encore, a Type Ia SN at $z = 1.949$, has a similar spectrum compared to those of local SNe, suggesting no cosmic evolution for the use of SNe Ia as a cosmological probe.

In this paper, we present a characterisation of SN 2025wny, the first galaxy-scale strongly lensed SN, which turns out to be a superluminous SN (SLSN). Its spatially resolved multiple images and time delays make it suitable for high-precision cosmography. In Sect. 2, we summarise the discovery and key properties of the supernova and lens system. Sect. 3 describes follow-up imaging, and Sect. 4 presents follow-up spectroscopy. We present redshift determinations for SN 2025wny and the second lens galaxy along with the SN classification in Sect. 5. Finally, we present a summary and outlook in Sect. 6.

2. SN 2025wny discovery

The Zwicky Transient Facility (ZTF; Bellm et al. 2019) first detected SN 2025wny on August 27, 2025 (ID ZTF25abnjznp), but the Gravitational-wave Optical Transient Observer (GOTO; Dyer et al. 2024) team first reported it to the Transient Name Server (TNS) on September 1, 2025 (ID GOTO25gqt). Based on Liverpool Telescope observations on October 3, 2025 (MJD 60951.21), the source was reported as a likely strongly lensed transient at RA = $07h\,16m\,34.500s$ and DEC = $+38d\,21m\,08.11s$, designated AT 2025wny (Wise et al. 2025). Three point-like images were identified within ∼2 arcsec from the strong lens candidate PS1 J0716+3821 (reported by our team, where we specifically searched for wide-separation lens systems as potential hosts of lensed transients that would be useful for cosmology; Cañameras et al. 2020), and photometry of the brightest multiple image (A, see Fig. 1) yielded magnitudes of $g = 20.42 \pm 0.04$, $r = 19.60 \pm 0.03$, and $i = 19.54 \pm 0.03$ (Wise et al. 2025).

The deflector is composed of a main lens and a smaller perturber galaxy, respectively labelled as G1 and G2 in Fig. 2. Wide-field imaging (from e.g. Pan-STARRS1, Chambers et al. 2016; Legacy Surveys DR9, Dey et al. 2019; and see Fig. 1) shows that the lens system lies in a rich environment (see also Fig. 3), with tens of galaxies exhibiting similar colours and photometric redshifts. Archival data from the Canada-France-Hawaii Telescope (CFHT; Gwyn 2012) from 2005 revealed four lensed images of the SN host galaxy in a cusp-like configuration (Fig. 3). The redshift of G1 has been spectroscopically confirmed by the Dark Energy Spectroscopic Instrument (DESI; Levi et al. 2013; DESI Collaboration et al. 2016) at $z_{\rm d} = 0.3754$, while G2 has a photometric redshift of $z_{\rm p,phot} = 0.32$ from the Dark Energy Camera Legacy Survey (DECaLS) DR9 imaging (Zhou et al. 2023).

Our team identified the transient as a possible lensed SN by cross-matching our lens-candidate list with Lasair (Smith et al. 2019) on September 21, 2025. Given its match with PS1 J0716+3821, SN 2025wny is the first detection of a wide-separation, galaxy-scale strongly lensed SN resulting from the search approach presented by Cañameras et al. (2020), which comprised (i) the systematic classification of all 3 billion sources detected in the Pan-STARRS 3π survey with deep learning, (ii) the selection of high-quality strong-lens candidates, and (iii) their continuous positional cross-matching with the public ZTF alert stream. Here, we present our first follow-up imaging and spectroscopic data, which we obtained despite a series of technical and meteorological obstacles.

3. Follow-up imaging

After identifying SN 2025wny as a promising lensed-SN candidate, we triggered follow-up imaging on September 29, 2025, at the Lulin Observatory (see Sect. 3.1) and on October 15, 2025, at the Maidanak Observatory (see Sect. 3.2). In addition, we started monitoring with a two- to three-day cadence using the 1.3 m COLIBRI telescope (Basa et al. 2022)[1] on October 15, 2025, in the *rz* bands, which was later extended to the *riz* bands. The 2.5 m Wide Field Survey Telescope (Wang et al. 2023) started observing SN 2025wny every two to three nights in the *ugr* filters on October 8, 2025, and the 1 m telescope at the Altay Observatory contributes *gri*-band observations. Finally, we started weekly imaging observations in *grizJ* with the Three Channel Imager (3KK; Lang-Bardl et al. 2016) mounted on the 2.1 m Fraunhofer Telescope at Wendelstein Observatory (Hopp et al. 2014). We provide a brief overview of the first imaging data below, while full details will be presented in a forthcoming publication once the imaging campaigns are completed. At that time, we will also provide all the magnitude measurements, the full light curves, and the measured time delays between the different strongly lensed images.

3.1. Lulin Observatory

We began our first imaging campaign on September 29, 2025, with the Lulin One-meter Telescope (LOT) at the Lulin Observatory as part of the DETECT (DESI Transient Event Cross-matching Tool) program (Y.-H. Lee et al., in prep.). Since then, we have obtained multiple epochs of *gri*-band imaging. The images were reduced following a standard procedure using a customised pipeline,[2] including bias subtraction, dark correction, and flat-fielding. Figure 1 shows the first *r*-band image taken on September 29, 2025, obtained under good observing conditions (full width at half maximum, $\mathrm{FWHM_r} = 1.04$ arcsec) with an exposure time of 10 min. We used AutoPhOT (Brennan & Fraser 2022) to perform the template subtraction. A difference image between this new observation and a Pan-STARRS1 image, serving as a template image without the lensed transient, clearly reveals the three transient images A, B, and C, and a marginal detection of image D (see Fig. 1, right panel). Therefore, this observation confirms that SN 2025wny is indeed strongly lensed. We measured *r*-band AB magnitudes of 19.6 mag, 21.3 mag, 21.5 mag for images A, B, and C, respectively.

3.2. Maidanak Observatory

Starting from October 15, 2025, we expanded our monitoring campaign by using the 1.5 m telescope of the Maidanak Observatory (Uzbekistan) (Ehgamberdiev 2018). We obtained imaging data in the *V*, *R*, and *I* filters (Im et al. 2010), each with

[1] COLIBRI is a Franco-Mexican telescope at the Observatorio Nacional Astronómico San Pedro Mártir, Baja California, México, in operation since January 2025.

[2] https://hdl.handle.net/11296/98q6x4

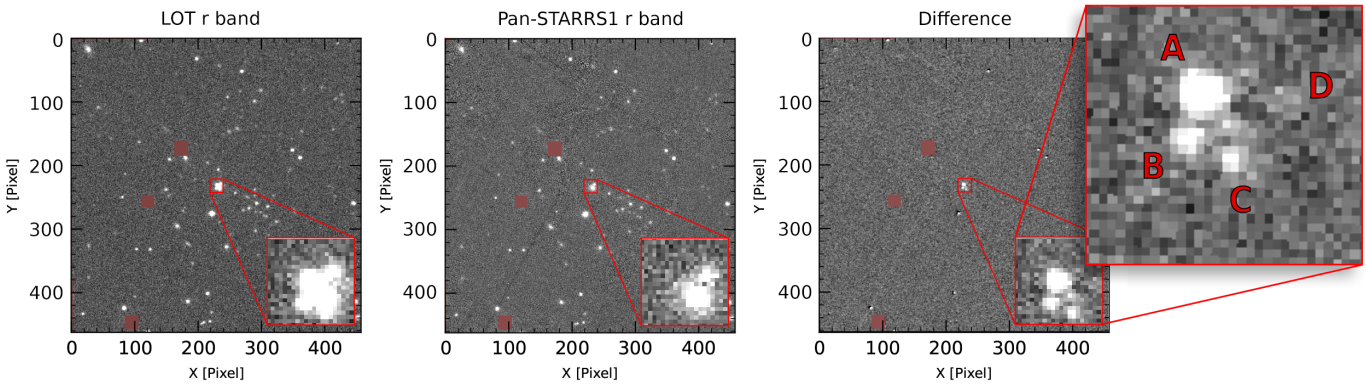

Fig. 1: Image of SN 2025wny in the *r*-band obtained at the Lulin Observatory with LOT on September 29, 2025 (left), Pan-STARRS1 reference image (middle), and difference image after subtraction (right). Very bright stars have been masked. The images cover an area of roughly 9 arcmin^2, with north being up and east to the left. The SN images A to D are labelled on a zoomed-in view of the difference image. Image A is located at RA = $07^h\,16^m\,34.500^s$ and DEC = $+38^d\,21^m\,08.11^s$.

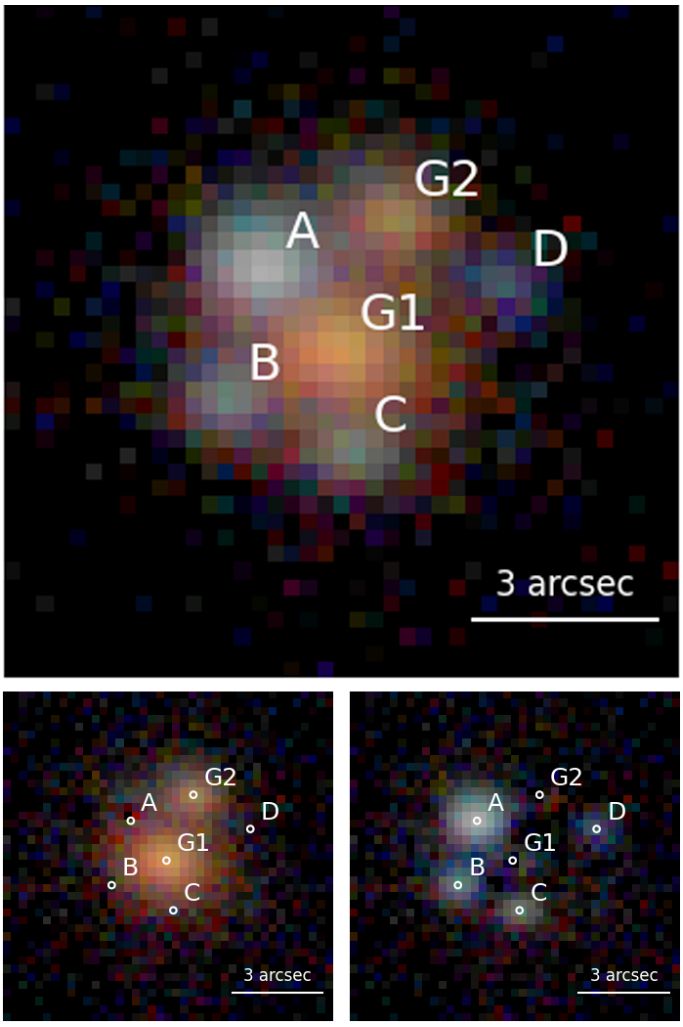

Fig. 2: Colour composite *VRI*-band image of SN 2025wny obtained at the Maidanak Observatory. The four visible SN images are labelled A, B, C, and D (in order of decreasing brightness), and the two foreground deflector galaxies are indicated as G1 and G2. Top: Observed image. Bottom left: The deflectors after subtracting SN and host light using Moffat profiles (with joint shape parameters). Bottom right: The SN images after subtracting the light of G1 and G2 using a single Sérsic profile each.

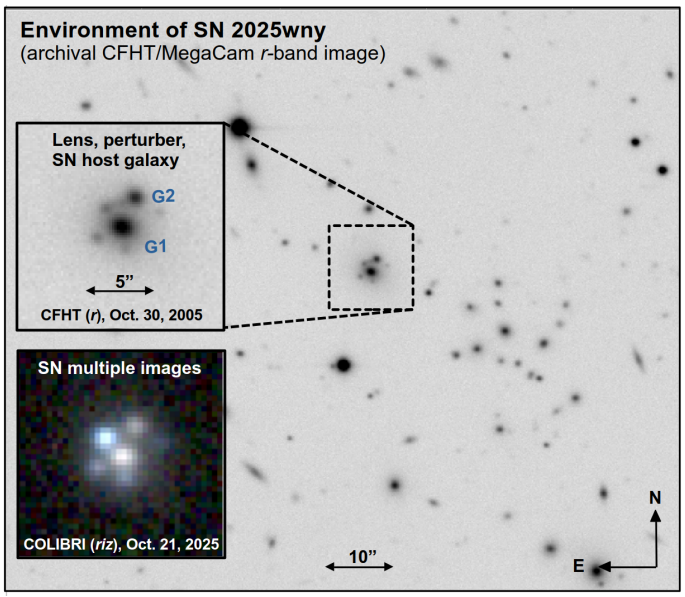

Fig. 3: Archival CFHT image from 2005 (Gwyn 2012) showing the two deflector galaxies G1 and G2 and the four strongly lensed images of the SN host galaxy. A colour image generated from COLIBRI-telescope *riz*-band data is included to facilitate comparison between the positions and brightnesses of the different SN and host-galaxy images.

about 30 min exposure time. Figure 2 (top) shows a colour composite of our first epoch of *VRI* data obtained under very good seeing conditions ($FWHM_V$ = 0.96 arcsec, $FWHM_R$ = 0.72 arcsec, $FWHM_I$ = 0.83 arcsec). In the bottom-left panel of Fig. 2, we show the light of the lens galaxies G1 and G2, and in the bottom-right panel, we show the SN (plus host) images only.

We measured *V*-, *R*-, and *I*-band Vega magnitudes of 20.31 ± 0.02 mag, 19.48 ± 0.01 mag, and 19.17 ± 0.01 mag for image A using point spread function (PSF) photometry with Moffat functions (Moffat 1969). The reference star used for the photometric calibration is at RA = $07^h\,16^m\,34.78^s$ DEC = $+38^d\,20^m\,51.0^s$, with magnitudes of G = 17.781, BP = 18.538, and RP = 16.858 from Gaia DR3 (Gaia Collaboration et al. 2021). We transformed the Gaia magnitudes into the Johnson-Cousins system using the equations from Riello et al. (2021). The uncertain-

ties were estimated based on the background noise and the PSF fitting residuals and are purely statistical. The reported magnitudes include some contamination from the underlying SN host galaxy, but given the brightness of SN image A relative to the host, the host contribution is at most a few percent. Difference-imaging magnitudes as well as magnitudes for the remaining images and for galaxies G1 and G2 will be presented in a forthcoming paper.

4. Spectroscopic observations with NOT and UH88

Optical spectroscopy of SN 2025wny image A was obtained with the 2.56 m Nordic Optical Telescope (NOT) + ALFOSC as part of the NOT Un-biased Transient Survey 2 (NUTS2[3]) programme on October 11, 2025 (MJD 60959.16). Two exposures of 1800 s each were taken with grism 4 and the 1.0 arcsec slit, resulting in a wavelength range from 3300 to 9700 Å and a spectral resolution of R $\sim$ 350. The slit was aligned along the parallactic angle, which serendipitously included part of the perturber galaxy (G2 in Fig. 2), for which no spectroscopic redshift was known before.

The data were reduced following standard procedures in IRAF[4] followed by an optimal, variance-weighted extraction of the spectra with the IRAF task `apall`. Wavelength calibration was accomplished with a HeNe arc-lamp spectrum and checked against night-sky emission lines. A spectrum of the spectrophotometric standard star BD+17d4708, obtained during the same night with an identical setup, was used for flux calibration and telluric correction. We checked the flux calibration against the Maidanak photometric observations of October 15 (Sect. 3.2) and found that the synthetic colours match the observed ones at the 2% level.[5]

A second spectrum with the NOT + ALFOSC was obtained on October 19, 2025 (MJD 60967.18), thanks to contributed programmes 68-804 and 71-804. This time, grism 18 was used in combination with the 1.0 arcsec slit to achieve a higher resolution of R $\sim$ 1000 for the blue part of the spectrum (3450 − 5350 Å). The slit was aligned to include images A and C, and the exposure time was 2×2400 s. The data reduction was carried out in the same way as for grism 4, with the standard star He 3 used for flux calibration. Both spectra are shown in Fig. 4.

Additionally, integral field spectroscopy (IFS) of the SN 2025wny system was obtained on October 16, 2025 (MJD 60963.59), with the University of Hawaii 88-inch Telescope (UH88) and the SuperNova Integral Field Spectrograph (SNIFS; Lantz et al. 2004). SNIFS has a microlens array of 15×15 spaxels, each $0.43 \times 0.43\,\mathrm{arcsec}^2$, giving a total field of view of $6.4 \times 6.4\,\mathrm{arcsec}^2$. This covers the entire SN 2025wny system, so the exposures contain the four SN images and the two lensing galaxies. The light is divided into blue (B) and red (R) channels, nominally spanning 3300 − 5150 Å and 5100 − 9700 Å, respectively. The corresponding spectral resolutions are 5.2 Å and 7.2 Å. Four exposures of 30 min each were obtained, during which the seeing was in the range 1.1 − 1.3 arcsec FWHM (which is somewhat worse than usual due to a warm primary mirror following an extended telescope shutdown). The combination of passing cirrus and moonlight further lowered the signal-to-noise ratio (S/N).

The SNIFS pipeline takes associated arcs and flats and constructs a 3D data cube of α, δ, λ. Whereas PSF photometry is usually used to extract SNe after subtracting a reference data cube obtained a year or more later (Bongard et al. 2011), this was not possible at this stage, so aperture extraction was used instead. To optimise the S/N and minimise the impact of position errors while avoiding contamination from the lensing galaxy and other sources, a 2 arcsec diameter aperture (i.e. a radius of $\sim$0.8 FWHM) was used (Howell 1989; King et al. 2013). The aperture locations were set separately for the B and R channels, but they were not corrected for atmospheric differential refraction as a function of wavelength within a channel. The maximum effect of this simplification is well below the noise and can be removed altogether in a future analysis that includes a reference data cube or model for the lensing galaxy. With each spectral extraction, the variance spectrum was estimated from the photon statistics and detector noise. As the S/N was similar for all four spectra, they were summed to produce the spectrum shown in Fig. 4. Flux calibration and telluric corrections used the pipeline defaults (Buton et al. 2013). Note that for this provisional reduction, the dichroic crossover region between 5000 and 5400 Å has not been fully corrected. Here, we show the spectral extraction only for image A, as the others yielded much lower S/N values and also had stronger contamination from the lensing galaxy.

5. Results

5.1. The redshift of SN 2025wny

Measuring the redshift of SN 2025wny turned out to be challenging at first since with the broad, blended spectral features in the blue part and the almost featureless continuum above $\sim$7000 Å (observer frame) in our NOT spectrum of October 11, 2025, the correct SN classification was not immediately obvious (see Fig. 4). The only constraint from strong lensing with a deflector at $z_\mathrm{d} = 0.375$ was that the redshift of the transient was most likely $\gtrsim 0.5$. Various SN classification codes (SNID, Blondin & Tonry 2007; GELATO, Harutyunyan et al. 2008; NGSF, Howell et al. 2005; Goldwasser et al. 2022) were used to classify the transient, but they all failed to provide compelling matches due to the lack of comprehensive spectral databases of SNe in the rest-frame UV.

Therefore, the key to the SN redshift could only come from narrow absorptions in the interstellar medium of the SN host galaxy. The most prominent narrow absorption in our NOT spectrum of October 11, 2025, is located at 4663 Å, and while it is not resolved, its FWHM is larger than expected for a single line. The most obvious guess for the nature of this line was Mg II $\lambda\lambda$2796, 2803, which would have set the SN at a redshift of $z = 0.665$. To verify or reject this hypothesis, we obtained a higher-resolution spectrum on October 19, 2025, in which the feature is clearly separated into two absorptions. The separation, however, which we measured to be $\sim$7 Å, is smaller than the $\sim$12 Å expected for Mg II. A convincing match was finally found for C IV $\lambda\lambda$1548, 1551 at $z_\mathrm{SN} = 2.008 \pm 0.001$, which is further supported by the detection of C II $\lambda\lambda$1335, 1336 and the unresolved Mg II $\lambda\lambda$2796, 2803 at the same redshift (Fig. 4, bottom panels).

[3] `https://nuts.sn.ie/`

[4] NOIRLab IRAF is distributed by the Community Science and Data Center at NSF NOIRLab, which is managed by the Association of Universities for Research in Astronomy (AURA) under a cooperative agreement with the U.S. National Science Foundation.

[5] This is not to claim that our photometry and spectral flux calibration reach this level of accuracy.

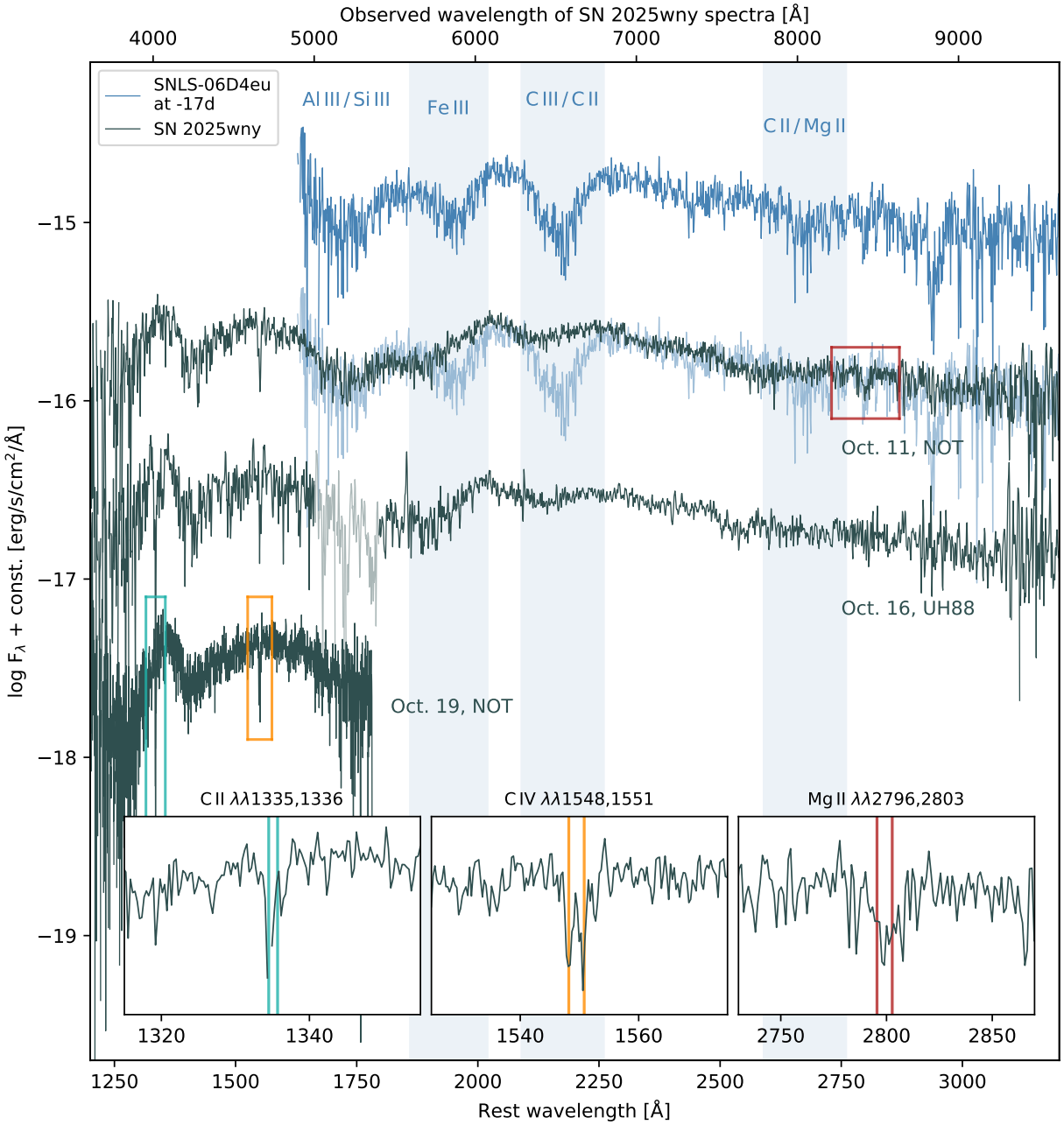

Fig. 4: Spectra of SN 2025wny obtained with NOT + ALFOSC and UH88 + SNIFS. A spectrum of the SLSN-I SNLS-06D4eu from Howell et al. (2013) is included for comparison, plotted once with and once without an offset relative to the SN 2025wny spectrum of October 11. SNLS-06D4eu provides the best match with SN 2025wny. Line identifications for SNLS-06D4eu have been adopted from Howell et al. (2013) and Mazzali et al. (2016), but we note that in SN 2025wny, the absorptions marked by the blue-shaded bands are weaker and more strongly blueshifted. The three inserts at the bottom of the image show zoom-ins on narrow absorption lines from the ISM in the host of SN 2025wny. We used them to determine the redshift of the SN, which is $z_{\rm SN} = 2.008 \pm 0.001$.

5.2. The redshift of the perturber galaxy

Besides the redshift of the strongly lensed SN also the redshift $z_{\rm p}$ of the second deflector galaxy G2 (the perturber) was previously unknown. Until now, only a photometric redshift estimate of $z_{\rm p,phot} = 0.32$ from DECaLS was available. However, accurately knowing the redshift of G2 is crucial for determining its effect on multiple image positions, lensing magnifications, and time delays. The fact that G2 was also included in the slit in the October 11 NOT spectrum allowed us to determine, for the first time, its spectroscopic redshift. Unfortunately, G2 is faint and was not perfectly centred in the slit, resulting in a low S/N of the extracted spectrum, yet the most important features of a passive-galaxy spectrum (Ca II H&K, Balmer break, G band, Mg I, Na I D) can be clearly identified. Fig. 5 shows the NOT spectrum with a Sloan Digital Sky Survey (SDSS) Data Release 5 (Adelman-McCarthy et al. 2007) template spectrum[6] of an early-type galaxy overlaid. From this match, we infer a

[6] https://classic.sdss.org/dr5/algorithms/spectemplates/

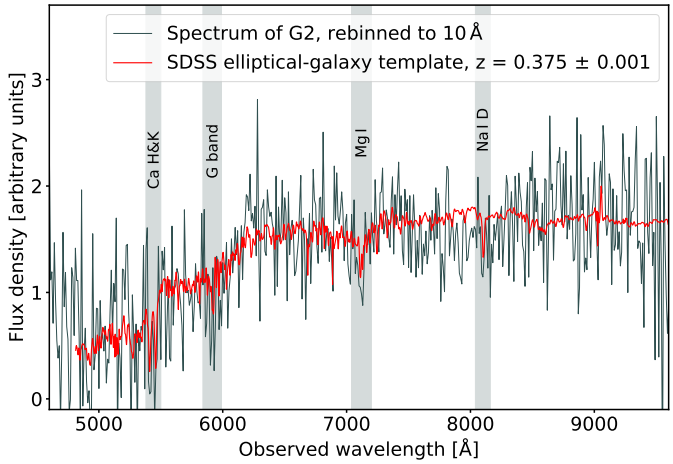

Fig. 5: October 11 NOT spectrum of the second deflector galaxy G2 ('perturber'), rebinned to a 10 Å bin size. An SDSS DR5 template spectrum of an early-type galaxy shifted to a redshift of $z_p = 0.375 \pm 0.001$ is superimposed. Ca II H&K, the Balmer break, the G band, Mg I, and Na I D are clearly detected.

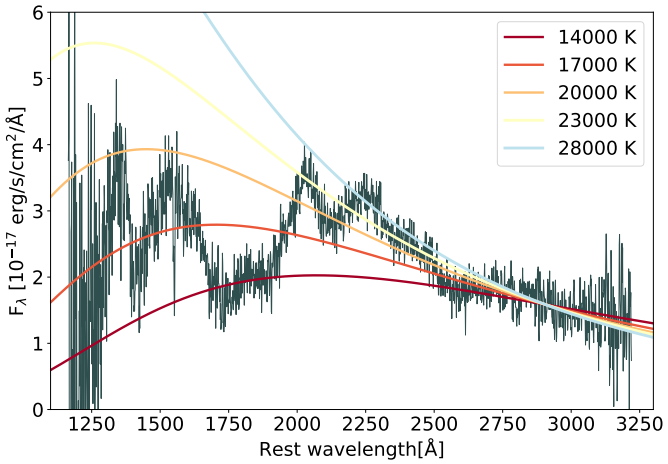

Fig. 6: Spectrum of SN 2025wny of October 11, 2025, with blackbody spectra for different temperatures overlaid. The spectra have been normalised at 2900 Å. An exact determination of the ejecta temperature is hampered by the strong and broad spectral features blueward of 2000 Å and the fact that the true continuum likely departs from a blackbody function. Still, we tentatively favour a temperature $\gtrsim 17\,000$ K.

redshift $z_p = 0.375 \pm 0.001$ for the perturber G2, where the uncertainty reflects the S/N of the NOT spectrum, the fact that the core of G2 was not centred in the slit, and possible inaccuracies in the wavelength calibration. The redshift of G2 is fully consistent with the spectroscopic redshift of the main lens G1. Hence, these two galaxies likely form a physical system.

5.3. A particularly UV-bright superluminous SN

With the redshift established, we continued our quest of determining the true identity of SN 2025wny. At $z_{SN} = 2.008 \pm 0.001$, the entire observed optical spectrum probes the rest-frame UV. Clearly there is no strong UV flux suppression or line blanketing as for most conventional SN types, especially SNe Ia. Instead, the spectral energy distribution (SED) peaks between 1300 and 2300 Å (rest-frame wavelength). A comparison of the October 11 spectrum to blackbody curves (Fig. 6) suggests very high ejecta temperatures of at least ∼17 000 K. Moreover, since the spectrum was taken 45 observer-frame days after discovery, corresponding to 15 rest-frame days, the high temperatures and UV flux were not just observed for a brief moment shortly after the explosion but persisted for several weeks.

The only class of SNe consistent with these characteristics are SLSNe, especially SLSNe-I. These objects, which were first identified as a distinct class by Quimby et al. in 2011, are usually explained by the explosion of very massive stars or the formation and subsequent spin-down of a magnetar (e.g. Inserra et al. 2013). They are UV-bright during their entire rise and around their peaks, a phase that often lasts for about 30 − 50 days (e.g. Gomez et al. 2024). Below 2000 Å, they are typically one to two orders of magnitude more luminous than other SN types, even when normalised to the same flux at optical wavelengths (see, e.g. Fig. 8 of Yan et al. 2017). Their peak absolute magnitudes at rest-frame optical wavelengths typically range from −20 to −22.5 (Gomez et al. 2024), which makes them observable even at large distances. Accordingly, photometrically typed SLSNe-I have been observed out to a redshift $z \sim 4$ (Cooke et al. 2012), whereas for spectroscopically confirmed events, the record holders are DES16C2nm at a redshift $z = 1.998$ (Smith et al. 2018), with several high-S/N spectra, and HSC16adga at $z = 2.399$ (Curtin et al. 2019), whose redshift and classification are on more shaky grounds given the extremely low S/N. With our spectroscopically confirmed redshift of 2.008 ± 0.001, SN 2025wny is therefore among the most distant spectroscopically confirmed SLSNe, making this a prime example of how strong lensing can help study transients that would otherwise be mostly out of reach.

We note that SN 2025wny is somewhat special among SLSNe-I, as it features an unusually smooth UV spectrum. The part between 2200 and 3200 Å is particularly featureless – a region where most SLSNe-I show several prominent broad spectral lines (e.g. Howell et al. 2013; Yan et al. 2017). However, as shown in Fig. 4, we do find a convincing spectral match with the SLSN-I SNLS-06D4eu (Howell et al. 2013), whose spectral features redward of 2200 Å are also strongly depressed. With a peak absolute magnitude of $M_U = -22.7$ and its high UV flux, SNLS-06D4eu is quite extreme even by SLSN standards. Howell et al. (2013) estimated a blackbody temperature of 13 500 – 14 000 K at the time the spectrum was taken (17 rest-frame days prior to the U-band peak), implying an SED peak of around 2100 Å. However, this may actually be an underestimate. In the wavelength region that SNLS-06D4eu and SN 2025wny have in common, the continuum overlaps very well (Fig. 4), but the SN 2025wny spectrum reaches further into the UV thanks to its higher redshift and shows significant emission below 1700 Å, thus favouring blackbody temperatures $\gtrsim 17\,000$ K to be properly reproduced (Fig. 6). A higher temperature is also supported by spectral modelling of SNLS-06D4eu by Mazzali et al. (2016), who inferred a blackbody temperature of 18 000 K, the highest among their sample of SLSNe-I.

The main spectral differences between SNLS-06D4eu and SN 2025wny concern the strengths and positions of three spectral lines near 1900, 2200, and 2700 Å (marked by blue-shaded bands in Fig. 4). These lines are significantly shallower and more strongly blueshifted in SN 2025wny. Howell et al. (2013) employed SEDONA radiative-transfer calculations (Kasen et al.

2006) of chemically homogeneous ejecta to identify these features as blends of mostly carbon lines, with contributions from magnesium and iron. Mazzali et al. (2016) largely confirmed this identification. However, they found a smaller contribution from singly ionised carbon due to the high temperature. They further attributed the feature near 1700 Å to resonance lines of doubly ionised aluminium and silicon. This feature is strong regardless of the overall ejecta composition since it already forms at a solar metal abundance (Howell et al. 2013). Howell et al. (2013) showed that the entire UV spectrum of SNLS-06D4eu can be well reproduced with a composition that is a mix of carbon and oxygen, with a solar admixture of heavier elements. Helium-dominated ejecta do not show the prominent carbon features and lead to an overall smoother appearance since all helium lines in the respective wavelength range turn out to be weak at the given density and temperature (see Fig. 12 of Howell et al. 2013).

This finding might actually be key to understanding the differences between SNLS-06D4eu and SN 2025wny. If the ejecta in SN 2025wny were more helium-rich and had a lower abundance of carbon and oxygen, the weakness of the carbon lines could be explained naturally. Alternatively, the differences in the strength of particular lines and their position could also arise from higher ejecta velocities in SN 2025wny or from a phase mismatch since we do not yet have sufficiently good photometric coverage to determine the phase of image A of SN 2025wny.

5.4. The odds of finding a strongly lensed superluminous SN

In the local Universe, superluminous SNe are extremely rare, but Prajs et al. (2017) showed that their rate increases with redshift, which is also consistent with the finding that their host galaxies are predominantly metal poor (e.g. Chen et al. 2013). However, even at $z \sim 1$, their rate is only a few times 10^{-4} of the volumetric rate of core-collapse SNe at the same redshift (Prajs et al. 2017; Frohmaier et al. 2021). Given this extreme rarity, one might wonder whether the detection of a strongly lensed SLSN is just a remarkable coincidence (reminiscent of the first gravitational wave detection of a neutron star merger and its electromagnetic counterpart; Abbott et al. 2017) or whether one might expect to find them more regularly in strong-lensing systems in the future. Without going into any detailed rate calculations, which are beyond the scope of this paper, we want to lay out a few arguments regarding why strongly lensed SLSNe might be discovered more frequently than previously thought despite their low intrinsic rate:

- Firstly, SLSNe are by far the most luminous SNe. Even at rest-frame optical wavelengths, they are about 2 mag more luminous than typical SNe Ia.
- They are also extremely UV-bright before and around their peaks. Their UV–optical colours are $3 - 4$ mag bluer than those of SNe Ia (see, e.g. Fig. 8 of Yan et al. 2017). At $z \gtrsim 1.5$, the observed optical light corresponds to the rest-frame UV regime. Hence, optical transient surveys such as ZTF and the Rubin Observatory Legacy Survey of Space and Time (LSST) are biased to detect UV-bright transients at those redshifts.
- If we make a thought experiment and replace SN 2025wny by a normal SN Ia at the same location and redshift, its observed r-band peak would be $5 - 6$ mag fainter than that of SN 2025wny. Hence, even the highly magnified image A would peak around 25 mag, whereas images B to D would peak closer to 27 mag. This is much fainter than the 5σ detection limit of LSST in single frames ($\sim 23 - 24$ mag, depending on the band).
- Superluminous SNe have intrinsically slowly evolving light curves, which are stretched out even more due to time dilation at high redshift. It is therefore very unlikely to miss a strongly lensed SLSN because of bad weather, technical failures, or even the seasonal gap.
- Little is known about the rate of SLSNe beyond redshift 1, but based on extrapolation of the trend from lower-redshift rate studies, they arguably might be more common beyond that point.

Present simulations of lensed-SN rates and detection prospects in ongoing and future transient surveys (Oguri & Marshall 2010; Wojtak et al. 2019; Arendse et al. 2024; Bag et al. 2024; Dong et al. 2024) do not consider SLSNe as a class, probably due to their low volumetric rate. Following the discovery of SN 2025wny, repeating such calculations for SLSNe would certainly be warranted.

6. Summary and outlook

We have presented the first characterisation of SN 2025wny, the first confirmed galaxy-scale strongly lensed supernova with expected time delays of days to weeks. The system consists of four lensed SN images produced by a two-galaxy deflector (G1 + G2), and the spectrum of the transient is consistent with an SLSN at $z_{\rm SN} = 2.008 \pm 0.001$. The fact that an SLSN, despite being intrinsically rare among all types of SNe, is one of the first galaxy-scale lensed SN systems to be detected is likely due to selection effects. Given the current limiting depth of the ZTF survey, only the brightest SNe are expected to be spatially resolved and detected when strongly lensed.

We have also presented key information on the G1 + G2 system. The measured spectroscopic redshift for G2 ($z_{\rm p} = 0.375 \pm 0.001$) helps us understand its impact on the image positions, magnifications, and time delays, and is thus a critical ingredient for modelling this complex lens system.

The immediate priority regarding further follow-up observations of SN 2025wny is a continued high-cadence photometric monitoring to measure the time delays between the multiple SN images. Ongoing observations with Maidanak, Lulin, COLIBRI, and Wendelstein will deliver the required densely sampled light curves. In addition, spectral monitoring of the evolution of the multiple SN images can also be used to determine the time delays (e.g. Bayer et al. 2021; Johansson et al. 2021; Chen et al. 2024). High-resolution imaging of this system from adaptive-optics assisted ground-based facilities or space-based observatories will also be important for detailed lens mass modelling. Both the Hubble Space Telescope (Programme ID 17611; PI: Goobar) and the James Webb Space Telescope (Programme ID 5564; PI: Goobar) were triggered to obtain follow-up imaging and IFS (Wise et al. 2025). The combination of time delays, lens mass modelling, and lens environment analysis has the potential to provide an independent and competitive determination of the value of H_0.

With the discovery of this first galaxy-scale lensed SN system suitable for cosmography, we are entering a new and exciting era. The discovery demonstrates the effectiveness of our lensed SN search strategy in HOLISMOKES, which consists of identifying static strong-lens systems in imaging surveys, cross-matching them to transient alerts, and flagging the cross-matches as lensed SN candidates (Shu et al. 2018; Cañameras et al. 2020). With the imminent start of the LSST, we anticipate that approximately ten lensed SNe Ia per year will be discovered that are useful for cosmography (Arendse et al.

2024), and the combination of Euclid and LSST will be an effective way to find lensed SNe (Sainz de Murieta et al. 2024). A sample of ∼20 lensed SNe Ia will not only enable rigorous testing of the time-delay methodology applied to lensed quasars but will also yield a measurement of H_0 with a 1% uncertainty, which is crucial for resolving the Hubble tension (e.g. Suyu et al. 2024).

For future reference, we propose the name 'SN Winny' for SN 2025wny to make this interesting object easier to remember. The name 'Winny' arises from its designation and evokes warmth and companionship – a gentle light in the dark. Given its distant, radiant glow, we deem this name very appropriate.

We note that during the final preparation of this manuscript, a TNS AstroNote (Johansson et al. 2025b) and classification report (https://www.wis-tns.org/object/2025wny/classification-cert) were published that independently confirm our results on both the redshift and classification of SN 2025wny. Moreover, one day after this work appeared on arXiv, Johansson et al. (2025a) published a similar but independent analysis of SN 2025wny based on a separate dataset on the preprint server.

Acknowledgements. Each alphabetically ordered group of authors reflects equal contributions within the group.
AA acknowledges financial support through the Beatriz Galindo programme and the project PID2022-138896NB-C51 (MCIU/AEI/MINECO/FEDER, UE), Ministerio de Ciencia, Investigación y Universidades. AM acknowledges funding from the Deutsche Forschungsgemeinschaft (DFG, German Research Foundation) – SFB 1258 – 283604770. SS has received funding from the European Union's Horizon 2022 research and innovation programme under the Marie Skłodowska-Curie grant agreement No 101105167 — FASTIDIoUS. We acknowledge financial support through grant PRIN-MIUR 2020SKSTHZ and from the University of Milan for the Nordic Optical Telescope programmes P68-804 and P71-804. AG, SHS and EM thank the Max Planck Society for support through the Max Planck Fellowship for SHS. This work is supported in part by the Deutsche Forschungsgemeinschaft (DFG, German Research Foundation) under Germany's Excellence Strategy – EXC-2094 – 390783311. MM acknowledges support by the Swiss National Science Foundation (SNSF) through return CH grant P5R5PT_225598 and Ambizione grant PZ00P2_223738. TMR is part of the Cosmic Dawn Center (DAWN), which is funded by the Danish National Research Foundation under grant DNRF140. TMR and SM acknowledge support from the Research Council of Finland project 350458. TLK acknowledges support via a Warwick Astrophysics prize post-doctoral fellowship made possible thanks to a generous philanthropic donation. TWC, AA, YHL acknowledge the financial support from the Yushan Fellow Program by the Ministry of Education, Taiwan (MOE-111-YSFMS-0008-001-P1) and the National Science and Technology Council, Taiwan (NSTC grant 114-2112-M-008-021-MY3). SY acknowledges the funding from the National Natural Science Foundation of China under grant No. 12303046, the Startup Research Fund of Henan Academy of Sciences No. 242041217, and the Joint Fund of Henan Province Science and Technology R&D Program No. 235200810057. FC acknowledges the support of the SNSF. YS acknowledges the support from the China Manned Space Program with grant no. CMS-CSST-2025-A20 and the National Natural Science Foundation of China (Grant No. 12333001). The Observatory of Maidanak team gratefully acknowledges the financial support provided by the Ministry of Higher Education, Science and Innovation of the Republic of Uzbekistan under grant No. IL-5421101855. GA wishes to acknowledge support from the United States Department of Energy, Office of Science, under Contract No. DE-AC02-05CH11231. CPG acknowledges financial support from the Secretary of Universities and Research (Government of Catalonia) and by the Horizon 2020 Research and Innovation Programme of the European Union under the Marie Skłodowska-Curie and the Beatriu de Pinós 2021 BP 00168 programme, from the Spanish Ministerio de Ciencia e Innovación (MCIN) and the Agencia Estatal de Investigación (AEI) 10.13039/501100011033 under the PID2023-151307NB-I00 SNNEXT project, from Centro Superior de Investigaciones Científicas (CSIC) under the PIE project 20215AT016 and the program Unidad de Excelencia María de Maeztu CEX2020-001058-M, and from the Departament de Recerca i Universitats de la Generalitat de Catalunya through the 2021-SGR-01270 grant. This work was supported by the "Action Thématique de Physique Stellaire" (ATPS) of CNRS/INSU PN Astro cofunded by CEA and CNES. This work alse received support by the Agencia Estatal de Investigación (AEI), Ministerio de Ciencia, Innovación y Universidades, Spain, under the project CNS2023-144016, and co-funded by the European Union – NextGenerationEU. BS acknowledges the support of the French Agence Nationale de la Recherche (ANR), under grant ANR-23-CE31-0011 (project PEGaSUS). JDRP is supported by NASA through a Einstein Fellowship grant No. HF2-51541.001 awarded by the Space Telescope Science Institute (STScI), which is operated by the Association of Universities for Research in Astronomy, Inc., for NASA, under contract NAS5-26555. JJ acknowledges the support from National Natural Science Foundation of China (Grant No. 12393811), National Key R&D Program of China (Grant No. 2023YFA1608100), the Strategic Priority Research Program of the Chinese Academy of Science (Grant No. XDB0550300), and the Japan Society for the Promotion of Science (JSPS) KAKENHI grants JP22K14069. KCW is supported by JSPS KAKENHI Grant Numbers JP24K07089, JP24H00221.
This research was partly based on observations made with the Nordic Optical Telescope (programme IDs: P72-503, P68-804, and P71-804) owned in collaboration by the University of Turku and Aarhus University, and operated jointly by Aarhus University, the University of Turku and the University of Oslo, representing Denmark, Finland and Norway, the University of Iceland and Stockholm University at the Observatorio del Roque de los Muchachos, La Palma, Spain, of the Instituto de Astrofisica de Canarias. The data presented here were obtained in part with ALFOSC, provided by the Instituto de Astrofisica de Andalucia (IAA) under a joint agreement with the University of Copenhagen and NOT. This publication makes use of data collected at the Lulin Observatory, which is partly supported by the TAOvA program under the NSTC grant 114-2740-M-008-002. We thank the anonymous referee for their prompt report, which helped clarify several aspects of the manuscript.

References

Abbott, B. P., Abbott, R., Abbott, T. D., et al. 2017, ApJ, 848, L12
Adelman-McCarthy, J. K., Agüeros, M. A., Allam, S. S., et al. 2007, ApJS, 172, 634
Agrawal, A., Pierel, J. D. R., Narayan, G., et al. 2025, submitted to ApJ, arXiv:2510.07637
Arendse, N., Dhawan, S., Sagués Carracedo, A., et al. 2024, MNRAS, 531, 3509
Bag, S., Huber, S., Suyu, S. H., et al. 2024, A&A, 691, A100
Basa, S., Lee, W. H., Dolon, F., et al. 2022, in Society of Photo-Optical Instrumentation Engineers (SPIE) Conference Series, Vol. 12182, Ground-based and Airborne Telescopes IX, ed. H. K. Marshall, J. Spyromilio, & T. Usuda, 121821S
Bayer, J., Huber, S., Vogl, C., et al. 2021, A&A, 653, A29
Bellm, E. C., Kulkarni, S. R., Graham, M. J., et al. 2019, PASP, 131, 018002
Birrer, S., Shajib, A. J., Galan, A., et al. 2020, A&A, 643, A165
Blondin, S. & Tonry, J. L. 2007, ApJ, 666, 1024
Bongard, S., Soulez, F., Thiébaut, É., & Pecontal, É. 2011, MNRAS, 418, 258
Brennan, S. J. & Fraser, M. 2022, A&A, 667, A62
Buton, C., Copin, Y., Aldering, G., et al. 2013, A&A, 549, A8
Cañameras, R., Schuldt, S., Suyu, S. H., et al. 2020, A&A, 644, A163
Chambers, K. C., Magnier, E. A., Metcalfe, N., et al. 2016, arXiv e-prints, arXiv:1612.05560
Chen, B. H., Hashimoto, T., Goto, T., et al. 2022, MNRAS, 509, 1227
Chen, T.-W., Smartt, S. J., Bresolin, F., et al. 2013, ApJ, 763, L28
Chen, W., Kelly, P. L., Frye, B. L., et al. 2024, ApJ, 970, 102
Cooke, J., Sullivan, M., Gal-Yam, A., et al. 2012, Nature, 491, 228
Curtin, C., Cooke, J., Moriya, T. J., et al. 2019, ApJS, 241, 17
DESI Collaboration, Aghamousa, A., Aguilar, J., et al. 2016, arXiv e-prints, arXiv:1611.00036
Dey, A., Schlegel, D. J., Lang, D., et al. 2019, AJ, 157, 168
Dhawan, S., Johansson, J., Goobar, A., et al. 2020, MNRAS, 491, 2639
Dhawan, S., Pierel, J. D. R., Gu, M., et al. 2024, MNRAS, 535, 2939
Dong, J., Shu, Y., Li, G., et al. 2024, A&A, 689, A192
Dyer, M. J., Ackley, K., Jiménez-Ibarra, F., et al. 2024, in Society of Photo-Optical Instrumentation Engineers (SPIE) Conference Series, Vol. 13094, Ground-based and Airborne Telescopes X, ed. H. K. Marshall, J. Spyromilio, & T. Usuda, 130941X
Ehgamberdiev, S. 2018, Nature Astronomy, 2, 349
Frohmaier, C., Angus, C. R., Vincenzi, M., et al. 2021, MNRAS, 500, 5142
Frye, B., Pascale, M., Cohen, S., et al. 2023, Transient Name Server AstroNote, 96, 1
Gaia Collaboration, Brown, A. G. A., Vallenari, A., et al. 2021, A&A, 649, A1
Goldwasser, S., Yaron, O., Sass, A., et al. 2022, Transient Name Server AstroNote, 191, 1
Gomez, S., Nicholl, M., Berger, E., et al. 2024, MNRAS, 535, 471
Goobar, A., Amanullah, R., Kulkarni, S. R., et al. 2017, Science, 356, 291
Goobar, A., Johansson, J., Schulze, S., et al. 2023, Nature Astronomy, 7, 1098
Grillo, C., Pagano, L., Rosati, P., & Suyu, S. H. 2024, A&A, 684, L23
Gwyn, S. D. J. 2012, AJ, 143, 38
Harutyunyan, A. H., Pfahler, P., Pastorello, A., et al. 2008, A&A, 488, 383

Hopp, U., Bender, R., Grupp, F., et al. 2014, in Society of Photo-Optical Instrumentation Engineers (SPIE) Conference Series, Vol. 9145, Ground-based and Airborne Telescopes V, ed. L. M. Stepp, R. Gilmozzi, & H. J. Hall, 91452D
Howell, D. A., Kasen, D., Lidman, C., et al. 2013, ApJ, 779, 98
Howell, D. A., Sullivan, M., Perrett, K., et al. 2005, ApJ, 634, 1190
Howell, S. B. 1989, PASP, 101, 616
Im, M.-S., Ko, J.-W., Cho, Y.-S., et al. 2010, Journal of Korean Astronomical Society, 43, 75
Inserra, C., Smartt, S. J., Jerkstrand, A., et al. 2013, ApJ, 770, 128
Johansson, J., Goobar, A., Price, S. H., et al. 2021, MNRAS, 502, 510
Johansson, J., Perley, D. A., Goobar, A., et al. 2025a, ApJ, 995, L17
Johansson, J., Qin, Y.-J., Goobar, A., et al. 2025b, Transient Name Server AstroNote, 306, 1
Kasen, D., Thomas, R. C., & Nugent, P. 2006, ApJ, 651, 366
Kelly, P. L., Rodney, S., Treu, T., et al. 2023, Science, 380, abh1322
Kelly, P. L., Rodney, S. A., Treu, T., et al. 2015, Science, 347, 1123
King, R. R., Naylor, T., Broos, P. S., Getman, K. V., & Feigelson, E. D. 2013, ApJS, 209, 28
Lang-Bardl, F., Bender, R., Goessl, C., et al. 2016, in Ground-based and Airborne Instrumentation for Astronomy VI, Vol. 9908, SPIE, 1295–1302
Lantz, B., Aldering, G., Antilogus, P., et al. 2004, in Society of Photo-Optical Instrumentation Engineers (SPIE) Conference Series, Vol. 5249, Optical Design and Engineering, ed. L. Mazuray, P. J. Rogers, & R. Wartmann, 146–155
Levi, M., Bebek, C., Beers, T., et al. 2013, arXiv e-prints, arXiv:1308.0847
Liu, Y. & Oguri, M. 2025, Phys. Rev. D, 111, 123506
Mazzali, P. A., Sullivan, M., Pian, E., Greiner, J., & Kann, D. A. 2016, MNRAS, 458, 3455
Messa, M., Vanzella, E., Loiacono, F., et al. 2025, A&A, 694, A59
Meštrić, U., Vanzella, E., Upadhyaya, A., et al. 2023, A&A, 673, A50
Millon, M., Courbin, F., Bonvin, V., et al. 2020, A&A, 642, A193
Moffat, A. F. J. 1969, A&A, 3, 455
Moresco, M., Amati, L., Amendola, L., et al. 2022, Living Reviews in Relativity, 25, 6
Oguri, M. 2019, Reports on Progress in Physics, 82, 126901
Oguri, M. & Marshall, P. J. 2010, MNRAS, 405, 2579
Pascale, M., Frye, B. L., Pierel, J. D. R., et al. 2025, ApJ, 979, 13
Pierel, J. D. R., Arendse, N., Ertl, S., et al. 2023, ApJ, 948, 115
Pierel, J. D. R., Frye, B. L., Pascale, M., et al. 2024, ApJ, 967, 50
Pierel, J. D. R., Hayes, E. E., Millon, M., et al. 2025, submitted to ApJ, arXiv:2509.12301
Planck Collaboration, Aghanim, N., Akrami, Y., et al. 2020, A&A, 641, A6
Prajs, S., Sullivan, M., Smith, M., et al. 2017, MNRAS, 464, 3568
Quimby, R. M., Kulkarni, S. R., Kasliwal, M. M., et al. 2011, Nature, 474, 487
Refsdal, S. 1964, MNRAS, 128, 307
Riello, M., De Angeli, F., Evans, D. W., et al. 2021, A&A, 649, A3
Riess, A. G., Yuan, W., Macri, L. M., et al. 2022, ApJ, 934, L7
Rodney, S. A., Brammer, G. B., Pierel, J. D. R., et al. 2021, Nature Astronomy, 5, 1118
Sainz de Murieta, A., Collett, T. E., Magee, M. R., et al. 2024, MNRAS, 535, 2523
Shu, Y., Bolton, A. S., Mao, S., et al. 2018, ApJ, 864, 91
Smith, K. W., Williams, R. D., Young, D. R., et al. 2019, Research Notes of the AAS, 3, 26
Smith, M., Sullivan, M., Nichol, R. C., et al. 2018, ApJ, 854, 37
Suyu, S. H., Acebron, A., Grillo, C., et al. 2025, submitted to A&A, arXiv:2509.12319
Suyu, S. H., Bonvin, V., Courbin, F., et al. 2017, MNRAS, 468, 2590
Suyu, S. H., Goobar, A., Collett, T., More, A., & Vernardos, G. 2024, Space Sci. Rev., 220, 13
Suyu, S. H., Huber, S., Cañameras, R., et al. 2020, A&A, 644, A162
Suyu, S. H., Marshall, P. J., Auger, M. W., et al. 2010, ApJ, 711, 201
Tdcosmo Collaboration, Birrer, S., Buckley-Geer, E. J., et al. 2025, A&A, 704, A63
Treu, T., Suyu, S. H., & Marshall, P. J. 2022, A&A Rev., 30, 8
Vanzella, E., Calura, F., Meneghetti, M., et al. 2017, MNRAS, 467, 4304
Verde, L., Schöneberg, N., & Gil-Marín, H. 2024, ARA&A, 62, 287
Wang, T., Liu, G., Cai, Z., et al. 2023, Science China Physics, Mechanics, and Astronomy, 66, 109512
Wise, J., Perley, D., Goobar, A., Johansson, J., & McGrath, Z. 2025, Transient Name Server AstroNote, 296, 1
Wojtak, R., Hjorth, J., & Gall, C. 2019, MNRAS, 487, 3342
Wong, K. C., Suyu, S. H., Chen, G. C.-F., et al. 2020, MNRAS, 498, 1420
Yan, L., Quimby, R., Gal-Yam, A., et al. 2017, ApJ, 840, 57
Zhou, R., Ferraro, S., White, M., et al. 2023, J. Cosmology Astropart. Phys., 2023, 097

[1] Technical University of Munich, TUM School of Natural Sciences, Physics Department, James-Franck-Str. 1, 85748 Garching, Germany
[2] Max Planck Institute for Astrophysics, Karl-Schwarzschild-Str. 1, 85748 Garching, Germany
[3] Instituto de Física de Cantabria (CSIC-UC), Avda. Los Castros s/n, 39005 Santander, Spain
[4] INAF – IASF Milano, via A. Corti 12, I-20133 Milano, Italy
[5] Aix-Marseille Université, CNRS, CNES, LAM, Marseille, France
[6] Graduate Institute of Astronomy, National Central University, 300 Jhongda Road, 32001 Jhongli, Taiwan
[7] Dipartimento di Fisica, Università degli Studi di Milano, via Celoria 16, I-20133 Milano, Italy
[8] E.O. Lawrence Berkeley National Laboratory, 1 Cyclotron Road, Berkeley, CA 94720, USA
[9] Institute for Particle Physics and Astrophysics, ETH Zurich, Wolfgang-Pauli-Str. 27, CH-8093 Zurich, Switzerland
[10] Département de Physique Théorique, Université de Genève, 24 quai Ernest-Ansermet, CH-1211 Genève 4, Switzerland
[11] Tuorla Observatory, Department of Physics and Astronomy, University of Turku, FI-20014 Turku, Finland
[12] Cosmic Dawn Center (DAWN), Niels Bohr Institute, University of Copenhagen, Jagtvej 128, DK-2200 Copenhagen N, Denmark
[13] Université Côte d'Azur, Observatoire de la Côte d'Azur, CNRS, Laboratoire Lagrange, France
[14] V.N. Karazin Kharkiv National University, Kharkiv, Ukraine
[15] Ulugh Beg Astronomical Institute, 33 Astronomicheskaya St., Tashkent 100052, Uzbekistan
[16] European Southern Observatory, Karl-Schwarzschild-Str. 2, 85748, Garching, Germany
[17] Niels Bohr Institute, University of Copenhagen, Jagtvej 128, DK-2200 Copenhagen N, Denmark
[18] Institut de Ciències del Cosmos (ICCUB), Universitat de Barcelona (IEEC-UB), Martí i Franquès 1, 08028 Barcelona, Spain
[19] Institució Catalana de Recerca i Estudis Avançats (ICREA), Passeig de Lluís Companys 23, 08010 Barcelona, Spain
[20] Institut d'Estudis Espacials de Catalunya (IEEC), Edifici RDIT, Campus UPC, 08860 Castelldefels, Barcelona, Spain
[21] Samarkand State University, 15, University boulevard, 140104, Samarkand, Uzbekistan
[22] Department of Physics, University of Warwick, Gibbet Hill Road, Coventry CV4 7AL, UK
[23] School of Sciences, European University Cyprus, Diogenes Street, Engomi, 1516, Nicosia, Cyprus
[24] Purple Mountain Observatory, Chinese Academy of Sciences, Nanjing, Jiangsu, 210023, China
[25] National Astronomical Observatories, Chinese Academy of Sciences, Beijing 100101, China
[26] Institute for Gravitational Wave Astronomy, Henan Academy of Sciences, Zhengzhou 450046, Henan, China
[27] University Observatory Munich, Faculty of Physics, Ludwig-Maximilians-Universität, Scheinerstr. 1, 81679 Munich, Germany
[28] Excellence Cluster ORIGINS, Boltzmannstr. 2, 85748 Garching, Germany
[29] Space Telescope Science Institute, 3700 San Martin Drive, Baltimore, MD 21218, USA
[30] NASA Einstein Fellow
[31] Institute for Astronomy, University of Hawaii, Honolulu, HI 96822-1897, USA
[32] Center for Astrophysics | Harvard & Smithsonian, 60 Garden Street, Cambridge, MA 02138, USA
[33] Research Center for the Early Universe, Graduate School of Science, The University of Tokyo, 7-3-1 Hongo, Bunkyo-ku, Tokyo 113-0033, Japan
[34] Universidad Nacional Autónoma de México, Instituto de Astronomía, A.P. 70-264, 04510 Ciudad de México, México
[35] Aix-Marseille Université, CNRS/IN2P3, Centre de Physique des Particules de Marseille (CPPM), IPhU, Marseille, France
[36] Instituto de Astronomía, Universidad Nacional Autónoma de Méx-

ico, km 107 Carretera Tijuana-Ensenada, 22860 Ensenada, Baja California, México
[37] Institute of Space Sciences (ICE, CSIC), Campus UAB, Carrer de Can Magrans, s/n, 08193 Barcelona, Spain
[38] Department of Astronomy, University of Science and Technology of China, Hefei 230026, China
[39] National Astronomical Observatory of Japan, 2-21-1 Osawa, Mitaka, Tokyo 181-8588, Japan
[40] Instituto de Ciencias Nucleares, Universidad Nacional Autónoma de México, Apartado Postal 70-264, 04510 México, Ciudad de México, México
[41] The Oskar Klein Centre, Department of Astronomy, Stockholm University, Albanova University Center, SE 106 91 Stockholm, Sweden
[42] Facultad de Ciencias, Universidad Nacional Autónoma de México, Apartado Postal 70-264, 04510 México, Ciudad de México, México